Journal of Statistical Physics, Vol. 62, Nos. 5/6, 1991

A New Method for Determining Hydrodynamic Effects on the Collision of Two Spheres

Fred Gelbard,[1] Lisa A. Mondy,[1] and Steven E. Ohrt[1]

Received January 30, 1990; final September 28, 1990

A sphere falling in a fluid may collide with another sphere falling more slowly if, when the spheres are far apart vertically, the horizontal distance between their centers is less than or equal to a critical radius. Accurate prediction of aerosol particle coagulation requires a good understanding of this process. Previously reported optical techniques for measuring hydrodynamic effects on this phenomenon have inherent difficulties detecting grazing collisions and hence in determining the critical radius. In this work, a novel detection technique is demonstrated and it is shown that the critical radius may be determined from the sound generated by the collision of two spheres in a viscous liquid. The technique is shown to provide a more precise and decisive indication of when hard spheres collide.

KEY WORDS: Hydrodynamic effects on collisions; aerosol particle gravitational coagulation; acoustical detection of collisions.

1. INTRODUCTION

Aerosol particles and incipient rain drops, ranging from about 1 to 100 μm in radius, will settle at different rates depending on their size, shape, and material density. This differential settling may result in particle collisions in which the particles stick and/or coalesce to form new larger particles that settle faster than their precursors. This so-called process of gravitational coagulation is of importance for rain drop formation in clouds and nuclear reactor safety studies of radioactive aerosol particle removal.

In order to avoid the intractable mathematical problems of precise modeling of multiparticle gravitational coagulation, the basic phenomenon is reduced to the problem of two rigid spheres falling under gravity in a

[1] Sandia National Laboratories, P.O. Box 5800, Albuquerque, New Mexico 87185.

0022-4715/91/0300-0945$06.50/0

quiescent and unbounded fluid. The particle concentrations are assumed low enough such that each pair of approaching spheres is undisturbed by the presence of other spheres.

The objective is to determine the critical radius y_c. It is defined as the horizontal offset of the center of the lower sphere (with radius r) from the vertical line through the center of the upper sphere (with radius R) when the spheres are far apart vertically, such that a grazing collision will occur. If the upper sphere is initially at a horizontal distance greater than y_c, this sphere will pass the lower sphere without a collision taking place. If the spheres have the same material density, then in general $R > r$ for a collision to occur.

In the absence of hydrodynamic effects, y_c would be given by $r + R$. However, hydrodynamic forces oppose the collision and y_c is less than $r + R$ for most cases of interest. For convenience, a collision efficiency is defined to be the area through which the center of the upper sphere must pass for a collision, divided by the same area in the absence of hydrodynamic effects. Thus, the collision efficiency ε is defined by

$$\varepsilon = \frac{y_c^2}{(r+R)^2} \tag{1}$$

The collision efficiency is less than unity at low Reynolds number ($\mathrm{Re} = 2RV\rho/\mu$, where V is the velocity of the larger sphere, and ρ and μ are the fluid density and viscosity, respectively). A value of $\varepsilon > 1$ would indicate that "wake capture" was enhancing the collision process as the trailing sphere experienced less resistance to motion when falling in the wake of the leading sphere (ref. 25, p. 467, 477).

Much theoretical work has been reported on determining the collision efficiency. Exact solutions of the Navier–Stokes equations for the two-sphere problem are available in the limit of $\mathrm{Re} \to 0$ (refs. 30, 5, 20, 22, 23; ref. 25, p. 636). However, in this limit, which is given by Stokes' approximation, the two spheres should never come in contact with each other, due to the so-called lubrication forces at the small gap between the spheres.

In reality, aerosol particles do touch and agglomerate. Therefore, for gravitational coagulation, a more complete description is needed than that given by Stokes' approximation of the Navier–Stokes equations. Recognizing the limitations of Stokes' approximation, theorists have considered three other effects in describing the gravitational coagulation. First, noncontinuum effects for the interstitial fluid when the gap between the particles becomes very small have been included in some calculations.[9,16,14]

Second, as the gap between particles becomes very small, surface

deformation[27] and van der Waal forces may become important.[2,8] Davis[7] and Wen and Batchelor,[34] using the expressions for the pairwise interaction of particles in Stokes flow developed by Batchelor,[3] considered the effects of attractive van der Waals forces on particles of arbitrary size and density. Davis[7] showed that these forces have a greater influence in promoting the collisions of small particles in clouds than does non-continuum flow.

Finally, inertial forces cannot be ignored in the inherently unsteady problem describing the motion of two spheres approaching each other, even if the Reynolds numbers of the spheres in isolation are much less than unity. Furthermore, for larger particles with Reynolds numbers greater than unity, where Stokes' approximation is certainly invalid, no exact analysis is available on determining the hydrodynamic effect. In the two-sphere problem, the range of Re in which the Stokes' approximation is applicable evidently becomes much smaller than that for a single sphere at steady-state velocity. This is emphasized by the experimental work of Steinberger *et al.*,[29] who observed the motion of pairs of spheres of the same size and density falling along their line of centers, in which a significant deviation from Stokes behavior was seen at Re as small as 0.03.

Calculations including approximations for inertial effects have been reported. Klett and Davis[17] considered the effect of fluid inertia using a modified Oseen flow model for small but nonzero Re. Their calculated collision efficiencies for particles of density 1.0 g/cm^3 in air were in all cases larger than those calculated with Stokesian hydrodynamics. For particles similar in size and greater than about 40 μm in radius, the collision efficiency was predicted to be greater than one. This wake capture could produce collision efficiencies near the size ratio r/R of 1.0 that were almost two orders of magnitude larger than those predicted by Davis,[9] and near the size ratio r/R of 0.5 that were an order of magnitude larger than those predicted by Davis.[9] Lin and Lee[18] and Schlamp *et al.*[26] used numerical solutions to the Navier-Stokes equations and the superposition method (in which each sphere is assumed to move in the flow field created by the other falling in isolation) to estimate the effects of fluid inertia. They predicted even larger collision efficiencies than did Klett and Davis[17] when r was greater than about 30 μm.

For many practical applications involving the incorporation of gravitational coagulation into computer codes, a simple empirical correlation is needed. An early calculation of y_c was given by Fuchs,[11] who considered the problem of the collection of small particles by a large, stationary sphere. His analysis ignored the disturbance of flow about the large particle due to the presence of the smaller particles and hence ignored the lubrication forces entirely. Adaptations of Fuchs' original work are

embedded in some of the computer codes used for aerosol modeling by the nuclear reactor technology community.[24,10] The expression attributed to Fuchs is given by

$$\varepsilon_F = \frac{3}{2}\left[\frac{r}{R+r}\right]^2 \qquad (R>r) \tag{2}$$

Pruppacher and Klett (ref. 25, p. 377) modified Fuchs' work in a slightly different analysis and obtained

$$\varepsilon_{PK} = \frac{1}{2}\left[\frac{r}{R+r}\right]^2 \qquad (R>r) \tag{3}$$

Pruppacher and Klett, recognizing the very approximate nature of either expression, justified applications of Eq. (3) [which is a factor of three smaller than Eq. (2)], since it more closely matches the complicated computations by Davis[9] for the collision efficiency for particles largely disparate in size. However, when the particles become closer in size, Davis' results are yet another factor of three smaller than the results given by Eq. (3).

The wide range in the predictions of collision efficiencies indicates that data on the hydrodynamics of two-particle interactions would be useful. Especially useful would be the empirical determination of the effects of fluid and particle inertia at nonzero Re. Unfortunately, experiments using aerosols are impractical because it is difficult to observe trajectories of individual particles and almost impossible to set or measure the initial horizontal offset of two particles.[21] Rather, most aerosol studies give only integrated information on collision efficiencies and are subject to errors of 10–20% (ref. 25, p. 484). Furthermore, studies with aerosols also have difficulty isolating the hydrodynamic effect from effects due to turbulence, shear, Brownian motion, and surface forces, and also have difficulty in accurately measuring particle size. The results to date have been inconclusive; for example, some show the presence of wake capture[1,31] and others show collision efficiencies that are less than one in all cases.[35,4]

An alternate approach to studying aerosol particle gravitational coagulation is to use a hydrodynamically similar system of two relatively large solid spheres settling in a viscous liquid. The sphere diameters can be measured accurately and the other difficulties mentioned previously are essentially eliminated. Accurate particle tracking with photography in such a system has been reported.[28,15,19] Comparable Reynolds numbers may be obtained, but it is very difficult to duplicate the particle/fluid material density ratio of aerosol particles in air with a solid sphere in a liquid. However, Pruppacher and Klett (ref. 25, p. 467 and 477) have argued that the system

is similar as long as the particle/fluid material density ratio is relatively large, based on the results by Steinberger *et al.* at a density ratio of about nine.[29] But it is not clear how important it is to match this ratio, and in this work, for demonstration purposes, the ratio may be as small as two. Even with cautious extension of particle tracking methods to aerosol particles or rain drops, detection of a grazing collision and distinguishing that from a near miss is virtually impossible by visual means alone. Therefore, a new acoustical detection technique was developed to determine when spheres collide while falling freely in a liquid.

2. EXPERIMENT

Experiments have been performed in a large tank of glycerin with three pairs of spheres on the order of 1 cm in diameter. (The dimensions of the tank and spheres are given in Table I. The spheres were chosen to be as close to spherical as practical for meaningful comparisons with the theories, which assume perfect spheres. Obviously, perfect spheres cannot be obtained and some surface roughness is unavoidable.) This corresponds to the range of aerosol particle Reynolds numbers on the order of about 10. A hydrophone (purchased from International Transducer Corporation, Model ITC-6065C) mounted at the bottom of the tank is used to detect the acoustic wave resulting from a collision. Immersed inside the rectangular tank is a cylindrical insert with an inner diameter of 35.6 cm and a height of 152 cm. As discussed in Section 3, inserts of various diameters are used to assess wall effects.

The acoustic signals are amplified by a factor of 1000, and band pass filtering is used, allowing only frequencies between 0.6 and 10 kHz to be recorded on a personal computer-operated data acquisition system. The collision signals are typically about 2.5 kHz in frequency. The hydrophone has been tested with a small sound source in this frequency range and has been shown to be insensitive to the position of the source within the tank.

The personal computer also controls the initial radial distance between the two balls and the timing of their release by a moving-ball dropper. The pair of spheres to be tested are loaded via an inclined ramp to set positions under the surface of the liquid. Each ball is held there until the release of a timed solenoid valve allows it to fall into a guide, which drops it vertically. The size of each guide conforms to the size of the sphere. The guides are positioned with an accurate stepper-motor-driven screw. Software controls the motor such that the initial radial offset of the two guides varies in precise increments. Increments as small as 1×10^{-4} cm, the limit of the stepper motor, can be achieved. The positions can be verified with an attached micrometer. Videos of the balls as they were released have verified

Table I. Summary of Experimental Conditions and Results

Apparatus dimensions:		
Inner diameter	35.6 cm	
Height	152 cm	
Fluid properties:		
Material	Glycerin	Glycerin
Temperature	24.16 ± 0.35°C	24.79 ± 0.17°C
Viscosity	9.39 P	8.8 P
Density	1.26 g/cm^3	1.26 g/cm^3
Upper sphere:		
Material	Steel	Brass
Density	7.78 g/cm^3	8.52 g/cm^3
Reynolds no. (24.16°C)	13	Not performed
Reynolds no. (24.79°C)	Not performed	15
Velocity (24.16°C)	51 cm/sec	Not performed
Velocity (24.79°C)	Not performed	56 cm/sec
Diameter ($2R$)	1.91 cm	1.90 cm
AFBMA grade	25	200
Diameter tolerance	$<3 \times 10^{-4}$ cm	$<3 \times 10^{-4}$ cm
Sphericity	$<6.4 \times 10^{-5}$ cm	$<5 \times 10^{-4}$ cm
Roughness	$<3.8 \times 10^{-6}$ cm	$<2 \times 10^{-5}$ cm
Lower sphere:		
Material	Glass[a]	Sapphire[b]
Density	2.518 g/cm^3	3.987 g/cm^3
Diameter ($2r$)	1.27 cm	1.27 cm
Reynolds no. (24.16°C)	1.9	3.1
Reynolds no. (24.79°C)	2.0	Not performed
Velocity (24.16°C)	11 cm/sec	18 cm/sec
Velocity (24.79°C)	11 cm/sec	Not performed
AFBMA grade	25	25
Diameter tolerance	$<3 \times 10^{-4}$ cm	$<3 \times 10^{-4}$ cm
Sphericity	$<6.4 \times 10^{-5}$ cm	$<6.4 \times 10^{-5}$ cm
Roughness	$<3.8 \times 10^{-6}$ cm	$<3.8 \times 10^{-6}$ cm
Initial relative velocity with steel sphere (24.16°C)	40 cm/sec	33 cm/sec
Initial relative velocity with brass sphere (24.79°C)	45 cm/sec	Not performed
Results:		
Critical radius[c]		
Lower sphere	Glass	Sapphire
With steel sphere	0.67 ± 0.03 cm	0.73 ± 0.03 cm
With brass sphere	0.69 ± 0.02 cm	Not performed
ε (collision efficiency)		
Lower sphere	Glass	Sapphire
With steel sphere	0.18 ± 0.02	0.21 ± 0.01
With brass sphere	0.19 ± 0.01	Not performed

$\varepsilon_F = 0.24$
$\varepsilon_{PK} = 0.08$

[a] Purchased from Winsted Precision Ball Company, Winsted, Connecticut.
[b] Purchased from General Ruby and Sapphire Corporation, Newport Richey, Florida.
[c] The critical radius for all three pairs of spheres did not differ statistically at the 95% confidence level.

that they do not spin upon release. Video analysis also has confirmed that at early times in free flight the radial offset between spheres is within 0.01 cm of that set with the guides. Errors in the transformation between camera coordinates and real-space coordinates are the limiting factor in the determination of the positions once in free flight, so that the positioning may, in fact, be even closer to that set with the guides.

Terminal velocity is reached very quickly upon the balls' release. The release of the second (larger and faster-falling) sphere is timed so that collision will take place in the lower half of the tank to allow a large initial separation distance, but not so close to the bottom that end effects are significant.[12] The spheres are released such that the collision occurs at a distance from the bottom that is larger than the radius of the cylindrical insert. The initial vertical separation is greater than 50 times the radius of the larger sphere to allow for the flow to be fully developed around the smaller sphere.

The testing is fully automatic, with one pair of spheres being lifted from the bottom of the tank with an Archimedes screw device, loaded into the ball-dropper, released sequentially at known times and distances apart, and then, after the recording of data, the same pair lifted again. Because the spheres are released in the liquid, the spheres are in thermal equilibrium with it. The temperature of the liquid is recorded automatically throughout the experiments. Pauses are built into the experimental procedure so that disturbances in the liquid caused by any part of the ball-dropper loading are allowed to dissipate before releasing the balls and obtaining collision data. Besides convenience, the automation is important because the acoustic collision signals are very faint. Movement about the room or conversation among workers would overwhelm the collision signal. To further reduce background noise, the apparatus was set up in an isolated building located in a remote field which is several miles from traffic. The field is closed to personnel from about 5:30 pm to 6:30 am, and most of the data were taken during that time interval.

Because very slight differences in initial conditions can change the trajectories of the spheres and, hence, whether the two spheres have a grazing collision or a near miss, many tests are done at each initial offset. This provides a large statistical data base so that the mean critical radius can be determined with confidence. Each data collection cycle consists of sphere releases over a range of initial offsets, starting from a very small offset, where collision is always expected, to a very large offset, where collision is not expected. The critical radius y_{max} for each cycle is defined as the largest offset that produced an acoustic collision signal with an amplitude of over twice the background noise.

To date, acoustic signals have been recorded for over 1000 interactions

between a steel sphere (1.91 cm diameter) overtaking and colliding with a glass or sapphire sphere (1.27 cm diameter) in glycerin. For the third pair of spheres, a brass sphere (1.90 cm in diameter) was used to overtake and collide with a glass sphere (1.27 cm in diameter).

Figures 1 and 2 show the data from two typical cycles testing the collision between the steel and glass spheres. The x axis is time, measured backward from when the spheres hit the bottom of the tank. The y axis is the amplified and digitized voltage obtained from the hydrophone. The label below each signal trace in the figures signifies the cycle number. Cycles 51 and 54 are shown in Figs. 1 and 2, respectively. The initial radial offset, in 0.01-in. (0.025-cm) intervals, is indicated by the extension (i.e., AUTO54.25 would be data taken with an initial offset of 0.25 in.). For both figures the critical radius is 0.71 cm (the last signal is seen at 0.28 in.) for a steel sphere ($2R = 1.91$ cm and a density of 7.78 g/cm^3), and a glass sphere ($2r = 1.27$ cm and a density of 2.518 g/cm^3).

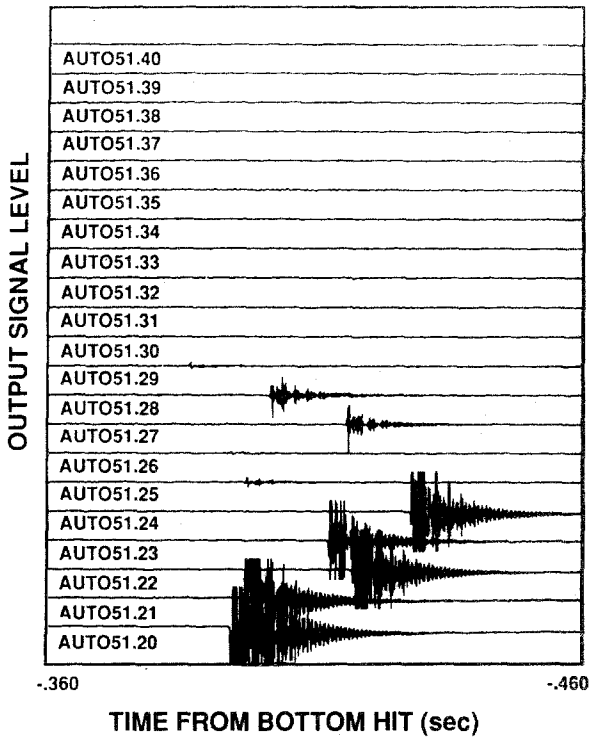

Fig. 1. Cycle 51 of acoustic signals obtained when a steel sphere (1.91 cm in diameter) collides with a glass sphere (1.27 cm in diameter), both in free fall in glycerin at 24.16 ± 0.35°C.

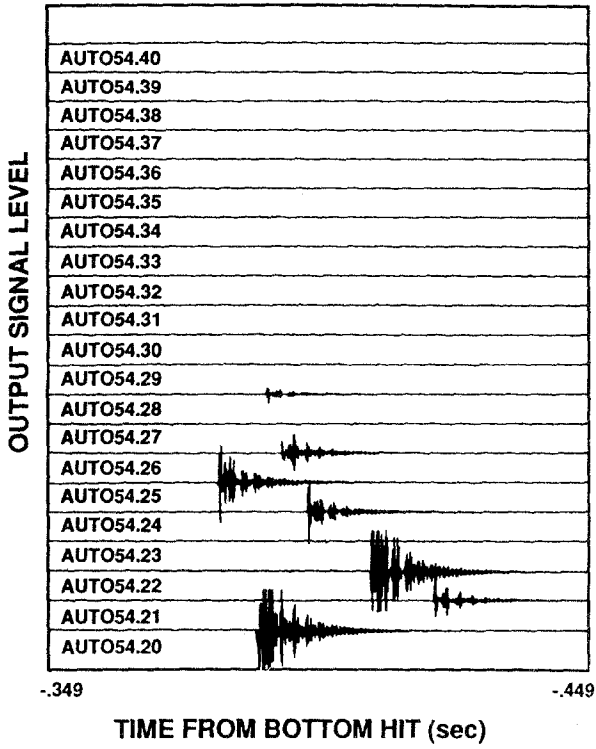

Fig. 2. Cycle 54 of acoustic signals obtained when a steel sphere (1.91 cm in diameter) collides with a glass sphere (1.27 cm in diameter), both in free fall in glycerin at 24.16 ± 0.35°C.

The first method used to determine y_c is to average the individual y_{max} measurements over many cycles. However, as seen in Figs. 1 and 2, often there are smaller offsets within a cycle which produce no signal. In order to examine the significance of these "gaps," a second method was also used to determine y_c. In this analysis, the probability (over many cycles) that a hit will occur at a certain offset was determined by summing the number of times a signal is produced and normalizing by the number of times the offset is tested. A plot of this probability distribution for collision of the steel and glass spheres is shown in Fig. 3. With a large data base, the probability that a signal will be produced decreases as the initial offset increases. The largest offset that produces a signal over 50% of the time is very close to the average critical radius as determined in the first method. In Fig. 4 the probability distribution for the brass and glass colliding is shown. Here the probability distribution decreases monotonically as the radial offset increases. Comparing Figs. 3 and 4, we see that the probability

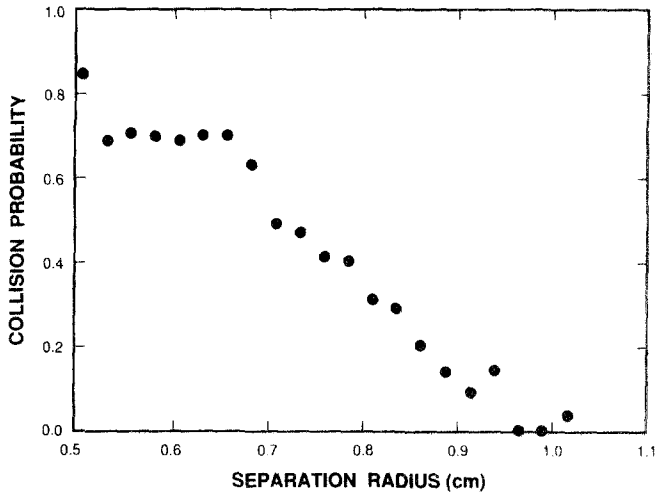

Fig. 3. Probability distribution of obtaining an acoustic signal of a collision as a function of the separation radius for a steel sphere (1.91 cm in diameter) colliding with a glass sphere (1.27 cm in diameter), both in free fall in glycerin at 24.16 ± 0.35°C.

distribution falls more precipitously in Fig. 4. Although the reason for this is not clear, it may be due to the differences between the steel and brass spheres, the improved temperature control, or the slightly higher temperatures used in the experiments with the brass and glass spheres.

The effect of the walls was reduced by carrying out the experiments in

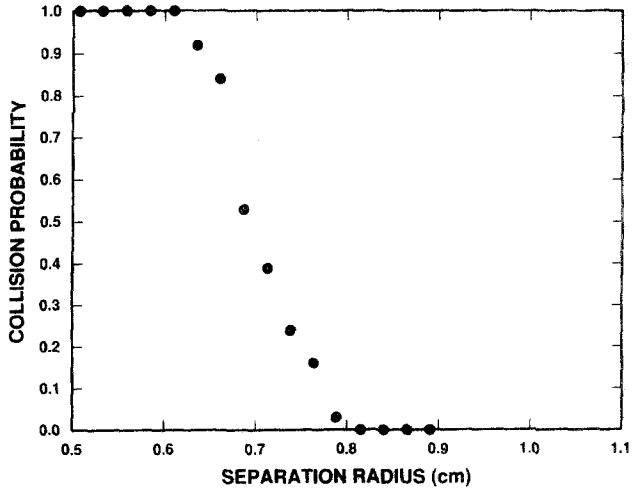

Fig. 4. Probability distribution of obtaining an acoustic signal of a collision as a function of the separation radius for a brass sphere (1.90 cm in diameter) colliding with a glass sphere (1.27 cm in diameter), both in free fall in glycerin at 24.79 ± 0.17°C.

a cylindrical insert of diameter 35.6 cm, which is large compared to the sphere diameters. The spheres were released as close to the axis of the cylinder as possible so that wall effects on the individual terminal velocities of the spheres could be calculated[6,13,12]; however, calculation of the effect on the interaction between the two spheres, like calculation of the critical radius itself, is mathematically intractable. Hence, wall effects were studied by varying the diameter of the tank by using various cylindrical inserts of inside diameters ranging from 11.6 to 35.6 cm.

With the smallest inserts, the critical radius increased dramatically. Spheres could be released with a large initial horizontal offset and an acoustic signal would be detected with the small inserts, but not with the larger inserts. Therefore, it appeared that the small inserts did not allow the free movement of the smaller sphere around the larger, forcing collisions at larger initial horizontal offsets. The critical radius decreased with increasing insert size, but more and more slowly, until little difference was observed between the critical radii obtained with the 30.5- and 35.6-cm-diameter inserts. Therefore, the wall effects on the critical radius are assumed to be negligible with the 35.6-cm-diameter insert and thus only data using this configuration are given in this work. However, the calculated Reynolds numbers and initial relative velocities given in Table I are corrected for wall effects.

3. RESULTS

Using the first method given above, over 26 cycles with the 1.91-cm-diameter steel and 1.27-cm-diameter glass spheres in glycerin at 24.16 ± 0.35, the measured critical radius was 0.67 ± 0.03 cm. The uncertainty is based on the 95% confidence limit for the Student t-test on the mean. The second method gives a probability of 0.63 of obtaining an acoustical signal at a radius of 0.68 cm and a probability of 0.49 at a radius of 0.71 cm. Based on a cutoff probability of 0.50, the critical radius would be about 0.68 cm, which is within the uncertainty of the first estimate. A plot of the measured probability distribution is given in Fig. 3, and a summary of the experimental conditions and results is given in Table I. (At this temperature, the viscosity of pure glycerin is 10.4 P. The measured viscosity, however, was 9.39 P, as determined from the time required for the glass ball to fall 25.4 cm and correcting for wall effects.[6,13] The difference in viscosity may be due to slight contamination by water.)

Based on the measured critical radius, using the first method, the collision efficiency as defined in Eq. (1) is 0.18 ± 0.02. Obviously, in this case no wake capture effect was observed, even at these large Reynolds numbers ($\mathrm{Re} = 13$ for the steel and $\mathrm{Re} = 1.9$ for the glass, falling in isolation). The

calculated relative velocity was about 40 cm/sec at large separation distances. Fuchs' expression [Eq. (2)], which was derived neglecting inertial effects (for Re much less than one), gives a collision efficiency of 0.24. It is interesting to note that this value comes closer to predicting the measured collision efficiency than do any of the more detailed models referenced above.

To explore possible variations of the critical radius with changes in the Reynolds number and the particle/fluid density ratio, two additional pairs of spheres were tested. In the second set of experiments, the glass sphere was replaced with a sapphire sphere of the same diameter (1.27 cm) and a material density of 3.987 g/cm^3. The calculated Reynolds number of the flow produced by the sapphire sphere falling in isolation was calculated to be about 3.1. The calculated relative velocity between the steel and sapphire spheres at large separation distances was about 33 cm/sec. In the third set of experiments, a brass sphere (1.90 cm in diameter) was tested with the glass sphere (1.27 cm in diameter) at a slightly higher temperature. The calculated relative velocity between the spheres at large separation distances was about 45 cm/sec.

Although Reynolds number, relative velocity, surface roughness, and particle/fluid density ratio were varied in the three sets of experiments, the critical radius did not differ statistically at the 95% confidence level. As mentioned in Section 1, there was concern that the critical radius may be sensitive to the particle/fluid density ratio, which ranged from 2.0 to 3.2, with the glass and the sapphire spheres, respectively. However, over this range, it does not appear that the collision efficiency is sensitive to this ratio. More data may reveal a small change as the statistical uncertainty in the average decreases.

Unfortunately, no acoustic signal could be detected at any initial separation distance for two sapphire spheres with diameters of 1.90 and 1.27 cm. Here, the calculated Reynolds numbers (6.8 and 3.0, respectively) are too large for Stokes flow to be valid. Perhaps there is a critical initial velocity difference below which either no collision takes place or below which the energy of the collision is too small to detect acoustically. The calculated relative velocity of this pair was 9 cm/sec. Further tests are planned with a variety of other sizes of spheres ranging from 0.64 to 2.5 cm in diameter.

4. DISCUSSION

The acoustical technique has a distinct advantage over visual interpretations of photographs in that either an unambiguous signal or no signal at all is observed. For the case when a signal is observed, it may be

questioned if that indeed signifies that a collision has occurred. One may argue that a thin film of fluid may still separate the spheres, but that film may allow an acoustical signal to be generated. Since the mechanism for sound generation is not clear, this question cannot be resolved completely. However, if a signal can be produced without direct contact, the remaining distance between the spheres is likely to be very small compared to the range over which attractive forces would dominate the interaction between aerosol particles.

In cases when no signal is detected, there are two possibilities: either the spheres did not collide (and no signal was generated) or a very small signal was generated that could not be observed with the equipment. The first possibility corresponds exactly to the desired characteristics of the measurement technique and needs no further consideration. The second possibility, however, needs to be addressed.

If no signal is detected because of the limited sensitivity of the measurement technique, then the collision efficiency is larger than that reported and would support Fuchs' expression even more. However, notice from Figs. 1 and 2 that the measurements do not indicate a gradual reduction in signal amplitude with increasing initial offset. Rather, the amplitude of the acoustic signal decreases very abruptly with increasing initial offset: a clear signal is detected or there is no signal at all. This abrupt change would probably occur even with more sensitive equipment because it is unlikely that, below the current sensitivity limit, the rate of change of the signal amplitude slows as the initial offset is increased. Therefore, it is unlikely that increased sensitivity would result in significantly different values of the measured critical radius.

As mentioned previously, y_{max} varies slightly for different cycles. Also, there sometimes are no signals where one is expected, which we previously referred to as "gaps." However, the variation in y_{max} between cycles is typically only a few hundredths of an inch. This is a small variation that can be attributed to very small, uncontrollable variations in setting the initial offset whose effects may be amplified as the spheres fall. These initially small perturbations are also believed to result in the observed gaps within a cycle. It is doubtful that the gaps are due to the hydrophone's sensitivity changing randomly. Therefore, the gaps are more readily explained if it is assumed that a collision always generates a detectable signal, but over a range of initial offsets a collision may or may not take place due to small changes in initial conditions.

The results do not indicate wake capture. In fact, for the collision efficiency to be equal to or greater than one in the present tests would require a collision at an initial offset about five times larger than the largest offset at which a signal was detected. Also, films of the process show it to

be exceedingly improbable that a collision could ever take place at this offset. (Since the camera generates too much noise, acoustic signal detection and filming could not be performed simultaneously. Instead, filming was performed in separate runs, but at the same temperature and offset used for the acoustic detection experiments.)

P. D. Thorne has measured the acoustic signals produced by the collision of spheres under water and has interpreted the results using rigid-body radiation theory.[32,33] The theory predicts a dependence, albeit weak, of the acoustic signal frequency on the relative velocity at the moment of collision. Using preliminary measurements of the frequency of our signals, Thorne predicts realistic values of the collision velocity (especially considering that there is a fairly large uncertainty in these frequency measurements due to limitations in the analog-to-digital data conversion of our current computer system). Future measurements may be able to provide not only measurements of the critical collision radius, but also more detailed information on the impact velocity during the collision.

5. CONCLUSIONS

A new acoustical technique for detecting the collision of hard spheres in a fluid has been demonstrated. For demonstration purposes, the technique was applied to the problem of determining the critical radius for a grazing collision to occur for two spheres falling freely in a viscous liquid. It was shown that acoustical detection in such a system could be used to support a theoretical model of gravitational coagulation. The best agreement with the measured collision efficiency came from the simple expression of Fuchs given by Eq. (2). Moreover, other models, such as Eq. (3), clearly lie outside the experimental data. Additional data are needed to substantiate this preliminary result.

ACKNOWLEDGMENT

This work was performed at Sandia National Laboratories, which is operated for the U.S. Department of Energy under contract DE-AC04-76DP00789.

REFERENCES

1. C. E. Abbott, Experimental cloud droplet collection efficiencies, *J. Geophys. Res.* **79**:3098 (1974).
2. M. K. Alam, The effect of van der Waals and viscous forces on aerosol coagulation, *Aerosol Sci. Technol.* **6**:41 (1987).

3. G. K. Batchelor, Sedimentation in a dilute polydisperse system of interacting spheres. Part 1. General theory, *J. Fluid Mech.* **119**:379 (1982).
4. K. V. Beard and H. R. Pruppacher, An experimental test of the theoretically calculated collision efficiency of cloud drops, *J. Geophys. Res.* **73**:6407 (1968).
5. H. Brenner, The slow motion of a sphere through a viscous fluid towards a plane surface, *Chem. Eng. Sci.* **16**:242 (1961).
6. R. Clift, J. R. Grace, and M. E. Weber, *Bubbles, Drops and Particles* (Academic Press, 1978), Chapter 9.
7. R. H. Davis, The rate of coagulation of a dilute polydisperse system of sedimenting spheres, *J. Fluid Mech.* **145**:179 (1984).
8. R. H. Davis, J. M. Serayssol, and E. J. Hinch, The elastohydrodynamic collision of two spheres, *J. Fluid Mech.* **163**:479 (1986).
9. M. H. Davis, Collision of small cloud droplets: Gas kinetic effects, *J. Atmos. Sci.* **29**:911 (1972).
10. I. H. Dunbar and J. Fermandjian, Comparison of sodium aerosol codes, Nuclear Safety ad Technology, Containment Loading and Response Safety Working Group Fast Reactor Coordinating Committee, Commission of the European Communities, ECI-878-B-7221-82UK (1984).
11. N. Fuchs, On the theory of overhead precipitation of warm clouds, *Dokl. Akad. Nauk SSSR* **81**:1043 (1951).
12. A. L. Graham, L. A. Mondy, J. D. Miller, N. J. Wagner, and W. A. Cook, Numerical simulations of eccentricity and end effects in falling ball rheometry, *J. Rheol.* **33**:1107 (1989).
13. J. Happel and H. Brenner, *Low Reynolds Number Hydrodynamics* (Martinus Nijhoff, Boston, 1973), Chapter 7.
14. L. M. Hocking, The effect of slip on the motion of a sphere close to a wall and of two adjacent spheres, *J. Eng. Math.* **7**:207 (1973).
15. V. G. Horguani, Determination of the trapping coefficient of cloud particles of comparable size by a model experiment, *Izv. Atm. Oceanic Phys.* **1**:208 (1965).
16. P. R. Jonas, The collision efficiency of small drops, *Q. J. R. Meteorol. Soc.* **98**:681 (1972).
17. J. D. Klett and M. H. Davis, Theoretical collision efficiencies of cloud droplets at small Reynolds numbers, *J. Atmos. Sci.* **30**:107 (1973).
18. G. L. Lin and S. C. Lee, Collision efficiency of water drops in the atmosphere, *J. Atmos. Sci.* **32**:1412 (1975).
19. S. K. Loyalka, R. C. Warder, W. Meyer, and T. S. Storvick, Experimental measurements of aerosol gravitational collision efficiency, *Trans. Am. Nucl. Soc.* **38**:401 (1987).
20. A. D. Maude, End effects in a falling-sphere viscometer, *Br. J. Appl. Phys.* **12**:293 (1961).
21. H. T. Ochs, R. R. Czys, and K. V. Beard, Laboratory measurements of coalescence efficiencies for small precipitation drops, *J. Atmos. Sci.* **43**:225 (1986).
22. M. E. O'Neill and S. R. Majumdar, Asymmetrical slow viscous fluid motions caused by the translation or rotation of two spheres. Part I: The determination of exact solutions for any values of the ratio of radii and separation parameters, *Z. Angew. Math. Phys.* **21**:164 (1970).
23. M. E. O'Neill and S. R. Majumdar, Asymmetrical slow viscous fluid motions caused by the translation or rotation of two spheres. Part II: Asymptotic forms of the solutions when the minimum clearance between the spheres approaches zero, *Z. Angew. Math. Phys.* **21**:180 (1970).
24. G. A. Pertmer and S. K. Loyalka, Gravitational collision efficiency of post hypothetical core disruptive accident liquid-metal fast breeder reactor aerosols: Spherical particles, *Nucl. Technol.* **47**:70 (1980).

25. J. R. Pruppacher and J. D. Klett, *Microphysics of Clouds and Precipitation* (D. Reidel, Dordrecht, Holland, 1980).
26. R. J. Schlamp, S. N. Grover, H. R. Pruppacher, and A. E. Hamielec, A numerical investigation of the effect of electric charges and vertical external electric fields on the collision efficiency of cloud drops, *J. Atmos. Sci.* **33**:1747 (1976).
27. J. M. Serayssol and R. H. Davis, The influence of surface interactions on the elastohydrodynamic collision of two spheres, *J. Colloid Interface Sci.* **114**:54 (1986).
28. R. M. Schotland, The collision efficiency of cloud drops of equal size, *J. Meteorol.* **14**:381 (1957).
29. E. H. Steinberger, H. R. Pruppacher, and M. Neiburger, On the hydrodynamics of pairs of spheres falling along their line of centres in a viscous medium, *J. Fluid Mech.* **34**:809 (1968).
30. M. Stimson and G. B. Jeffery, The motion of two spheres in a viscous fluid, *Proc. R. Soc. A* **111**:110 (1926).
31. J. W. Telford, N. S. Thorndike, and E. G. Bowen, The coalescence between small water drops, *Q. J. R. Meteorol. Soc.* **81**:241 (1955).
32. P. D. Thorne and D. J. Foden, Generation of underwater sound by colliding spheres, *J. Acoust. Soc. Am.* **84**:2144 (1988).
33. P. D. Thorne, Private communication (1989).
34 C. S. Wen and G. K. Batchelor, The rate of coagulation in a dilute suspension of small particles, *Sci. Sinica A* **28**:172 (1985).
35. J. D. Woods and B. J. Mason, The wake capture of water drops in air, *Q. J. R. Meteorol. Soc.* **91**:35 (1965).